

---

# Tutorial on Gabor Filters

---

Copyright © 1996,2002 Javier R. Movellan.

This is an open source document. Permission is granted to copy, distribute and/or modify this document under the terms of the GNU Free Documentation License, Version 1.2 or any later version published by the Free Software Foundation; with no Invariant Sections, no Front-Cover Texts, and no Back-Cover Texts.

## **Endorsements**

This document is endorsed by its copyright holder: Javier R. Movellan. Modified versions of this document should delete this endorsement.

## 1 The complex Gabor in space domain

Here is the formula of a complex Gabor function in space domain

$$g(x, y) = s(x, y) w_r(x, y) \quad (1)$$

where  $s(x, y)$  is a complex sinusoidal, known as the **carrier**, and  $w_r(x, y)$  is a 2-D Gaussian-shaped function, known as the **envelop**.

### 1.1 The complex sinusoidal carrier

The complex sinusoidal is defined as follows,<sup>1</sup>

$$s(x, y) = \exp(j(2\pi(u_0 x + v_0 y) + P)) \quad (2)$$

where  $(u_0, v_0)$  and  $P$  define the spatial frequency and the phase of the sinusoidal respectively.

We can think of this sinusoidal as two separate real functions, conveniently allocated in the real and imaginary part of a complex function (see Figure 1).

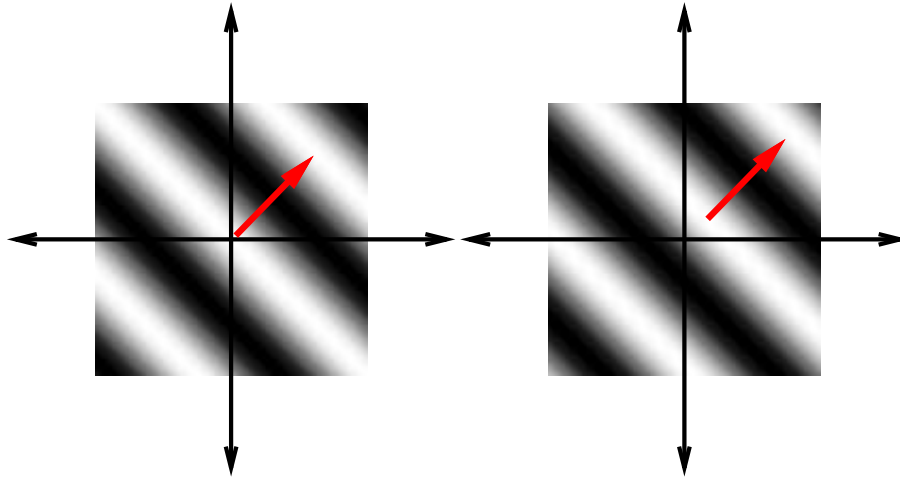


Figure 1: The real and imaginary parts of a complex sinusoidal. The images are  $128 \times 128$  pixels. The parameters are:  $u_0 = v_0 = 1/80$  cycles/pixel,  $P = 0$  deg.

---

<sup>1</sup>An offset constant parameter for  $s(x, y)$  will be introduced later, to compensate the DC-component of this sinusoidal. Refer to the appendix for detailed explanation.

The real part and the imaginary part of this sinusoidal are

$$\begin{aligned}\operatorname{Re}(s(x, y)) &= \cos(2\pi(u_0 x + v_0 y) + P) \\ \operatorname{Im}(s(x, y)) &= \sin(2\pi(u_0 x + v_0 y) + P)\end{aligned}\tag{3}$$

The parameters  $u_0$  and  $v_0$  define the spatial frequency of the sinusoidal in Cartesian coordinates. This spatial frequency can also be expressed in polar coordinates as magnitude  $F_0$  and direction  $\omega_0$ :

$$\begin{aligned}F_0 &= \sqrt{u_0^2 + v_0^2} \\ \omega_0 &= \tan^{-1}\left(\frac{v_0}{u_0}\right)\end{aligned}\tag{4}$$

*i.e.*

$$\begin{aligned}u_0 &= F_0 \cos \omega_0 \\ v_0 &= F_0 \sin \omega_0\end{aligned}\tag{5}$$

Using this representation, the complex sinusoidal is

$$s(x, y) = \exp(j(2\pi F_0(x \cos \omega_0 + y \sin \omega_0) + P))\tag{6}$$

## 1.2 The Gaussian envelop

The Gaussian envelop looks as follows (see Figure 2):

$$w_r(x, y) = K \exp\left(-\pi\left(a^2(x - x_0)_r^2 + b^2(y - y_0)_r^2\right)\right)\tag{7}$$

where  $(x_0, y_0)$  is the peak of the function,  $a$  and  $b$  are scaling parameters<sup>2</sup> of the Gaussian, and the  $_r$  subscript stands for a rotation operation<sup>3</sup> such that

$$\begin{aligned}(x - x_0)_r &= (x - x_0) \cos \theta + (y - y_0) \sin \theta \\ (y - y_0)_r &= -(x - x_0) \sin \theta + (y - y_0) \cos \theta\end{aligned}\tag{8}$$

## 1.3 The complex Gabor function

The complex Gabor function is defined by the following 9 parameters;

- $K$  : Scales the magnitude of the Gaussian envelop.
- $(a, b)$  : Scale the two axis of the Gaussian envelop.
- $\theta$  : Rotation angle of the Gaussian envelop.
- $(x_0, y_0)$  : Location of the peak of the Gaussian envelop.
- $(u_0, v_0)$  : Spatial frequencies of the sinusoidal carrier in Cartesian coordinates.  
It can also be expressed in polar coordinates as  $(F_0, \omega_0)$ .
- $P$  : Phase of the sinusoidal carrier.

Each complex Gabor consists of two functions in quadrature (out of phase by 90 degrees), conveniently located in the real and imaginary parts of a complex function.

---

<sup>2</sup>Note that the Gaussian gets smaller in the space domain, if  $a$  and  $b$  get larger.

<sup>3</sup>This rotation is clockwise, the inverse of the counterclockwise rotation of the ellipse.

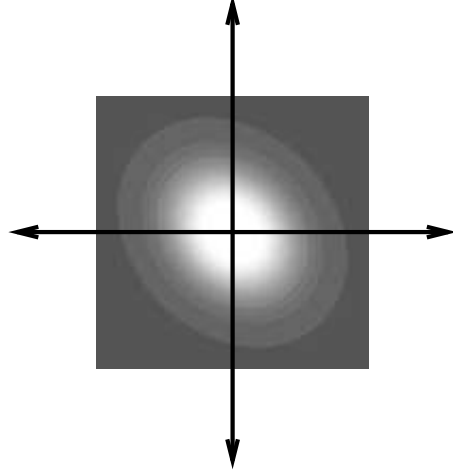


Figure 2: A Gaussian envelop. The image is  $128 \times 128$  pixels. The parameters are as follows:  $x_0 = y_0 = 0$ .  $a = 1/50$  pixels,  $b = 1/40$  pixels,  $\theta = -45$  deg.

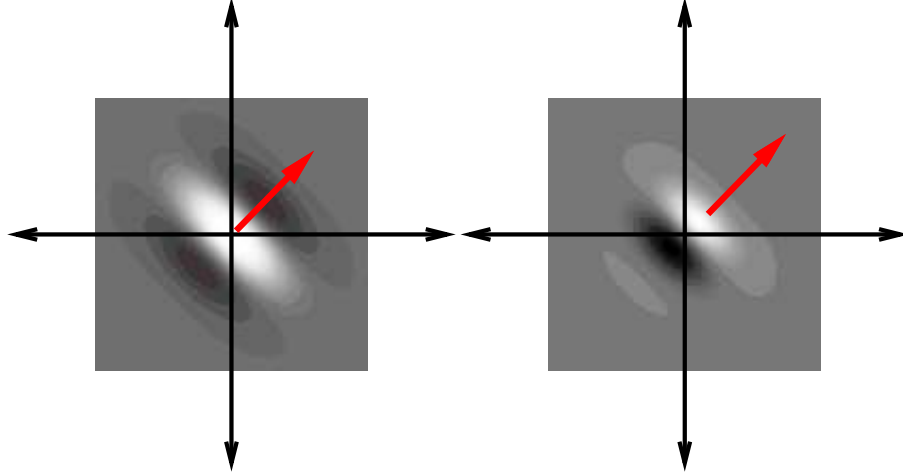


Figure 3: The real and imaginary parts of a complex Gabor function in space domain. The images are  $128 \times 128$  pixels. The parameters are as follows:  $x_0 = y_0 = 0$ ,  $a = 1/50$  pixels,  $b = 1/40$  pixels,  $\theta = -45$  deg,  $F_0 = \sqrt{2}/80$  cycles/pixel,  $\omega_0 = 45$  deg,  $P = 0$  deg.

Now we have the complex Gabor function in space domain<sup>4</sup> (see Figure 3):

$$g(x, y) = K \exp \left( -\pi \left( a^2 (x - x_0)_r^2 + b^2 (y - y_0)_r^2 \right) \right) \exp (j (2\pi (u_0 x + v_0 y) + P)) \quad (9)$$

---

<sup>4</sup>In fact, there remains some DC component in this Gabor function. You have to compensate it to have the admissible Gabor function. Refer to the appendix.

Or in polar coordinates,

$$g(x, y) = K \exp \left( -\pi \left( a^2 (x - x_0)_r^2 + b^2 (y - y_0)_r^2 \right) \right) \exp (j (2\pi F_0 (x \cos \omega_0 + y \sin \omega_0) + P)) \quad (10)$$

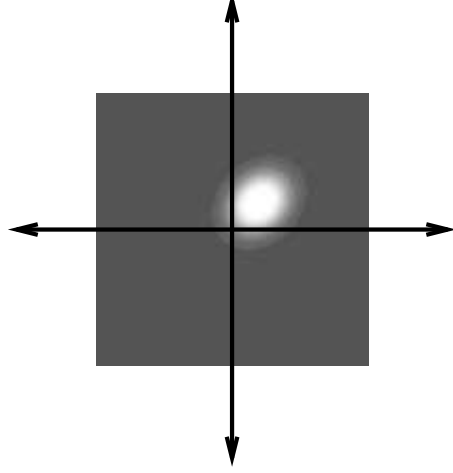


Figure 4: The Fourier transform of the Gabor filter. The peak response is at the spatial frequency of the complex sinusoidal:  $u_p = v_p = 1/80$  cycles/pixel. The parameters are as follows:  $x_0 = y_0 = 0$ ,  $a = 1/50$  pixels,  $b = 1/40$  pixels,  $\theta = -45$  deg,  $F_0 = \sqrt{2}/80$  cycles/pixel,  $\omega_0 = 45$  deg,  $P = 0$  deg.

The 2-D Fourier transform of this Gabor<sup>5</sup> is as follows (see Figure 4):

$$\begin{aligned} \hat{g}(u, v) = & \frac{K}{ab} \exp(j(-2\pi(x_0(u - u_0) + y_0(v - v_0)) + P)) \\ & \exp\left(-\pi\left(\frac{(u - u_0)_r^2}{a^2} + \frac{(v - v_0)_r^2}{b^2}\right)\right) \end{aligned} \quad (11)$$

Or in polar coordinates,

$$\begin{aligned} \text{Magnitude } (\hat{g}(u, v)) &= \frac{K}{ab} \exp\left(-\pi\left(\frac{(u - u_0)_r^2}{a^2} + \frac{(v - v_0)_r^2}{b^2}\right)\right) \\ \text{Phase } (\hat{g}(u, v)) &= -2\pi(x_0(u - u_0) + y_0(v - v_0)) + P \end{aligned} \quad (12)$$

---

<sup>5</sup>Refer to the appendix for detailed explanation.

## 2 Half-magnitude profile

The region of points, in frequency domain, with magnitude equal one-half the peak magnitude can be obtained as follows. Since the peak value is obtained for  $(u, v) = (u_0, v_0)$ , and the peak magnitude is  $K/ab$ , we just need to find the set of points  $(u, v)$  with magnitude  $K/2ab$ .

$$\frac{1}{2} \frac{K}{ab} = \frac{K}{ab} \exp \left( -\pi \left( \frac{(u - u_0)_r^2}{a^2} + \frac{(v - v_0)_r^2}{b^2} \right) \right) \quad (13)$$

or,

$$-\log 2 = -\pi \left( \frac{(u - u_0)_r^2}{a^2} + \frac{(v - v_0)_r^2}{b^2} \right) \quad (14)$$

or equivalently,

$$\left( \frac{(u - u_0)_r}{aC} \right)^2 + \left( \frac{(v - v_0)_r}{bC} \right)^2 = 1 \quad (15)$$

$$\text{where } C = \sqrt{\frac{\log 2}{\pi}} = 0.46971864 \approx 0.5$$

Equation 15 is an ellipse centered at  $(u_0, v_0)$  rotated with an angle  $\theta$  with respect to the  $u$  axis. The main axis of the ellipse have length  $2aC \approx a$  and  $2bC \approx b$  respectively.

We will use the following convention:  $a$  is the length of the axis closer to  $\omega_0$ , and  $b$  is the length of the axis perpendicular to the main axis<sup>6</sup> (See Figure 5).

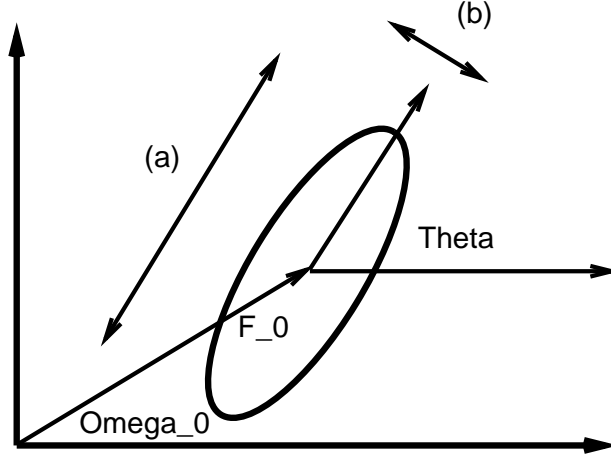


Figure 5: Parameters of the Gabor kernel as reflected in the half-magnitude elliptic profile. Note that this is a figure in frequency domain.

## 3 Half-magnitude frequency and orientation bandwidths

Frequency and orientation bandwidths of neurons are commonly measured in terms of the half-magnitude responses. Let  $u_0, v_0$  the preferred spatial frequency of a neuron. In polar coordinates this spatial frequency can be expressed as  $F_0$  and  $\omega_0$ .

<sup>6</sup>More precisely  $a$  and  $b$  are 1.06 times the length of the respective axis

To find the half-magnitude frequency bandwidth, we probe the neuron with sinusoidal images of orientation  $\omega_0$  and different spatial frequency magnitudes  $F$ . We increase  $F$  with respect to  $F_0$  until the magnitude of the response is half the magnitude at  $(F_0, \omega_0)$ . Let's call that value  $F_{\max}$ . We then decrease  $F$  with respect to  $F_0$  until the magnitude of the response is half the response at  $(F_0, \omega_0)$ . Call that  $F_{\min}$ . Half-magnitude frequency bandwidth is defined as follows:

$$\Delta F_{1/2} = F_{\max} - F_{\min} \quad (16)$$

or, when measured in octaves,<sup>7</sup>

$$\Delta F_{1/2} = \log_2 (F_{\max}/F_{\min}) \quad (17)$$

Half-magnitude orientation bandwidth is obtained following the same procedure but playing with the orientation  $\omega$  instead of the frequency magnitude  $F$ .

$$\Delta \omega_{1/2} = \omega_{\max} - \omega_{\min} \quad (18)$$

In Gabor functions with  $\theta_0 \approx \omega_0$  the frequency bandwidth can be obtained as follows (See Figure 6)

$$\Delta F_{1/2} = 2 a C \approx a \quad (19)$$

and the orientation bandwidth can be approximated as follows (see Figure 6)

$$\Delta \omega_{1/2} \approx 2 \tan^{-1} \left( \frac{b C}{F_0} \right) \quad (20)$$

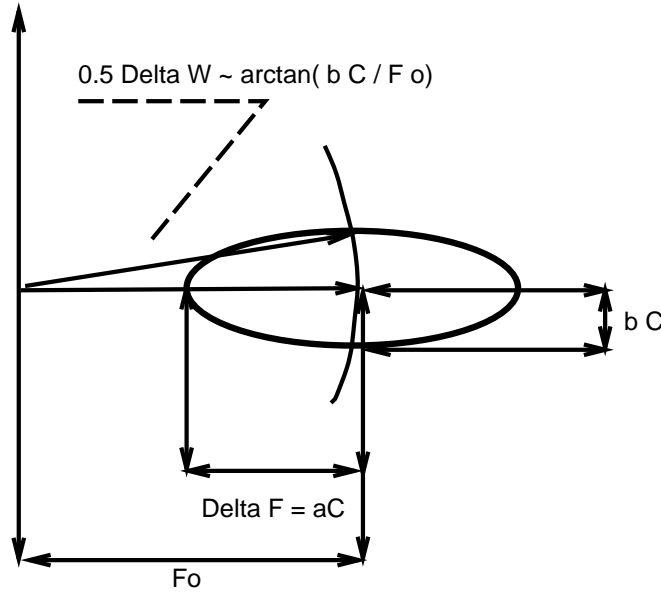


Figure 6: A half-magnitude profile and its relationship to the orientation and frequency bandwidths.

<sup>7</sup>Octave is a unit used for showing the ratio, as an index of 2.  $k$  octaves =  $2^k \times 100.0\%$



## 4 Effective spread and rms spread

The rms (which stands for root mean squares) length, rms width, and rms area of a 2-D function are defined in terms of their first and second moments:

The moments of a complex function  $g(x, y)$  are defined by converting the function into a probability density (which must be always positive and integrates to 1.0) and then calculating the standard first and second moments.

A common way to achieve this is as follows:

From the function  $g(x, y)$  we construct the following probability density

$$f(x, y) = \frac{1}{Z} |g(x, y)|^2 \quad (21)$$

where  $|g(x, y)|^2$  is the magnitude of the signal, which is always positive, and  $Z$  guarantees that  $f(x, y)$  integrates to 1.0, *i.e.*

$$Z = \int_{-\infty}^{+\infty} \int_{-\infty}^{+\infty} |g(x, y)|^2 dx dy \quad (22)$$

Once we have defined a probability density function, the standard statistical measures of location and scale follow.

$$\mu_X = E_X(x) = \int \int f(x, y) x dx dy \quad (23)$$

$$\sigma_X^2 = E_X((x - \mu_X)^2) = \int \int f(x, y) (x - \mu_X)^2 dx dy \quad (24)$$

with similar equations for  $\mu_Y$  and  $\sigma_Y^2$ .

$$\mu_Y = E_Y(y) = \int \int f(x, y) y dx dy \quad (25)$$

$$\sigma_Y^2 = E_Y((y - \mu_Y)^2) = \int \int f(x, y) (y - \mu_Y)^2 dx dy \quad (26)$$

And,

$$\sigma_{XY} = E_{XY}((x - \mu_X)(y - \mu_Y)) = \int \int f(x, y) (x - \mu_X)(y - \mu_Y) dx dy \quad (27)$$

The rms width and length are defined as the  $\sigma_X$  and  $\sigma_Y$  of a rotated version of  $f(x, y)$  so that the covariance  $\sigma_{XY}$  of the rotated distribution be zero.

Let  $X_r, Y_r$  represent the rotated variables for which the covariance is zero, the rms length and width are

$$\Delta X_{\text{rms}} = \sqrt{\sigma_{X_r}^2} \quad (28)$$

$$\Delta Y_{\text{rms}} = \sqrt{\sigma_{Y_r}^2} \quad (29)$$

Similar definitions can be obtained also in the frequency domain, by working with the Fourier transform of the original complex function.

$$\Delta U_{\text{rms}} = \sqrt{\sigma_{U_r}^2} \quad (30)$$

$$\Delta V_{\text{rms}} = \sqrt{\sigma_{V_r}^2} \quad (31)$$

The rms area in the space and frequency domains are defined as follows:

$$\text{Area}(XY)_{\text{rms}} = (\Delta X_{\text{rms}})(\Delta Y_{\text{rms}}) \quad (32)$$

$$\text{Area}(UV)_{\text{rms}} = (\Delta U_{\text{rms}})(\Delta V_{\text{rms}}) \quad (33)$$

Some papers work with what are known as effective length, width and areas. They are simply the rms measures multiplied by  $\sqrt{2\pi}$

$$\Delta X_{\text{eff}} = \sqrt{2\pi} \Delta X_{\text{rms}} \quad (34)$$

and so on.

It can be shown that the following relationships hold on any 2D function with finite moments

$$(\Delta X_{\text{rms}})(\Delta U_{\text{rms}}) \geq \frac{1}{4\pi} \quad (35)$$

$$(\Delta Y_{\text{rms}})(\Delta V_{\text{rms}}) \geq \frac{1}{4\pi} \quad (36)$$

and

$$\text{Area}(XY)_{\text{rms}} \text{Area}(UV)_{\text{rms}} \geq \frac{1}{16\pi^2} \quad (37)$$

It is easy to verify that the Gabor complex function achieves the lower limits of the uncertainty relations. For a given area in the space domain it provides the maximum possible resolution in the frequency domain, and vice-versa.

It can be shown that the rms width and lengths of Gabor functions are as follows:

$$\Delta U_{\text{rms}} = \frac{a}{2\sqrt{\pi}} \quad (38)$$

$$\Delta V_{\text{rms}} = \frac{b}{2\sqrt{\pi}} \quad (39)$$

To see why, simply consider that the probability density associated with the Gabor function  $f(x, y) = \frac{1}{Z} |g(x, y)|^2$  is Gaussian with variances equal to  $\Delta U_{\text{rms}}^2$  and  $\Delta V_{\text{rms}}^2$ .

Moreover, from the uncertainty relations,

$$\Delta X_{\text{rms}} = \frac{1}{2a\sqrt{\pi}} \quad (40)$$

$$\Delta Y_{\text{rms}} = \frac{1}{2b\sqrt{\pi}} \quad (41)$$

## 5 Gabor functions as models of simple cell receptive fields

Jones and Palmer (1987) showed that the real part of complex Gabor functions fit very well the receptive field weight functions found in simple cells in cat striate cortex.

Here are some of the constraints that can be found in the literature:

- The orientation of the Gaussian  $\omega_0$  is roughly equivalent to the orientation of the carrier.<sup>8</sup>  $\theta_0 = \omega_0$ . The absolute deviations, “the twist” have a Median of about 10 degrees (see Jones and Palmer, 1987, p. 1249).

---

<sup>8</sup>It's easier to consider in the frequency domain. Note that the long axis in the frequency domain becomes the short axis in the space domain. Don't get confused!

- In macaque V1, most cells have a spatial frequency bandwidth between 1 and 1.5 octaves. The median is about 1.4 octaves (see De Valois et al., 1982a, p. 551).
- Orientation bandwidths are typically about 40 degrees (mean = 65 degrees, median = 42 degrees, mode = 30 degrees) (see De Valois et al., 1982b, p. 535 and 541).
- From the three constraints mentioned above, it may be derived (see equation 59) that the aspect ratio is typically about 1.24, *i.e.*  $a/b \approx 1.24$ .
- In the area mapping the fovea, there are more kernels oriented vertically and horizontally than oriented diagonally (about 3 to 2). (see De Valois et al., 1982b, p. 537).
- Pairs of adjacent simple cells in the visual cortex of the cat are in quadrature (Pollen and Ronner, 1981). We can then put these two cells in the real and imaginary parts of a complex function and treat them as a complex Gabor receptive field.

## 6 Gabor functions for spatial frequency filtering

Consider a massive set of simple cell neurons with Gabor kernel functions with equal parameters except for the location parameters  $(x_0, y_0)$ . Let all these neurons be distributed uniformly about the foveal field. Each point in the foveal field contains at least two neurons in quadrature. We can model the operation of such a set of neurons as a convolution operation (assuming a continuous and uniform distribution of filters in all the foveal locations). Since convolution in space domain is product in frequency domain, the set of Gabor functions work as bandpass frequency filters of the foveal image. The peak frequency is controlled by the spatial frequency of the sinusoidal carrier  $(u_0, v_0)$ . The half-magnitude region is controlled by the rotation  $\theta$  and scale parameters  $a, b$ , of the Gaussian envelop.

## 7 Energy filtering

A quadrature pair (or a Hilbert Transform pair) is a set of two linear operators with the same amplitude response but phase responses shifted by 90 degrees. Strictly speaking sine and cosine Gabor operators are not quadrature pairs because cosine phase Gabors have some DC response, whereas sine gabors do not. However, one can have quadrature Gabor pairs that look very much like sine/cosine pairs. Thus the sine and cosine Gabor pair is commonly referred to as a quadrature pair.

A system that sums the square of the outputs of a quadrature pair is called an energy mechanism (Adelson and Bergen, 1985). Energy mechanisms have unmodulated responses to drifting sinusoidals.

Complex cells in V1 are commonly modeled as energy mechanisms since they are unmodulated by drifting sinusoidals. Simple cells respond to a drifting sinusoidal with a half-wave rectified analog of the signal, suggesting that the cells are linear up to rectification. Complex cells respond to a drifting sinusoidal in an unmodulated way, as a maintained discharge. Movshon et al. (1987) showed that complex receptive fields are composed of subunits. The subunits of model complex cells are model simple cells with identical amplitude response. Emerson et al. (1992) have shown that behavior of complex cell to stimuli made of pairs of bars flashed in sequence is consistent with an energy mechanism.

## 8 Contrast Normalization

Morrone et al. (1982) have shown that stimuli presented at orientations orthogonal to the optimal orientation inhibit simple cells activity. (De Valois et al., 1982a) have shown similar inhibitory effect between frequency bands. These inhibitory effects may play a serve as a gain control (or contrast normalization) mechanism. Heeger (1991) proposes the following model of gain control in complex cells: The amplitude response of each energy mechanism is divided by the total energy at all orientations and nearby spatial frequencies:

$$\bar{E}_i = \frac{E_i}{\kappa + \sum_j E_j} \quad (42)$$

where  $\kappa$  is a positive constant to avoid zero denominators.

## 9 Functional Interpretations

Section in preparation:

- minimizes number of neurons needed to achieve a desired frequency resolution.
- spatially and frequency localized.
- matched to “logons” likely to occur in images.
- for natural images the Gabor representation is more sparse than the  $\delta$  (pixel) representation and than the DOG representation.

## 10 Constructing an idealized V1

We’ll use the following simplified assumptions. They all have empirical support.

- The orientation of the complex sinusoid carrier and the Gaussian envelop are the same:  $\omega_0 = \theta$ .
- The half-magnitude frequency bandwidth is constant for all neurons when measured in octaves.
- The half-magnitude orientation bandwidth is constant for all neurons.
- The upper half-magnitude contour of a frequency band coincides with the lower contour of the next frequency band. This is just a constrain we use for convenience.

From these assumptions above, we can derive the relationship between the parameters  $F_0$ ,  $a$  and  $b$ .

From equations 17 and 19, we know that the frequency bandwidth in octaves is

$$\Delta F_{1/2} = \log_2 \frac{F_0 + aC}{F_0 - aC} \quad (43)$$

$$\text{where } C = \sqrt{\frac{\log 2}{\pi}} = 0.46971864 \approx 0.5$$

Thus,

$$a = F_0 \frac{K_a}{C} \quad (44)$$

where

$$K_a = \frac{2^{\Delta F} - 1}{2^{\Delta F} + 1} \quad (45)$$

With respect to the orientation bandwidth, equation 20 tells us that

$$\tan\left(\frac{1}{2}\Delta\omega\right) = \frac{bC}{F_0} \quad (46)$$

Thus,

$$b = F_0 \frac{K_b}{C} \quad (47)$$

where

$$K_b = \tan\left(\frac{1}{2}\Delta\omega\right) \quad (48)$$

Therefore, in this model the aspect ratio of  $a$  and  $b$  is constant:

$$\lambda = \frac{a}{b} = \frac{K_a}{K_b} \quad (49)$$

Moreover, from equation 19

$$\frac{1}{2}\Delta F = aC = F_0 K_a \quad (50)$$

We can now locate our frequency peaks such that the upper half-magnitude contour of one channel coincides with the lower half-magnitude contour of the the next channel.

Let  $\mu_i$  signify the peak frequency of the  $i^{th}$  band,

We know  $F_{\max}$  for band  $i$  is

$$F_{\max}^i = \mu_i + \frac{1}{2}\Delta F_i = \mu_i + \mu_i K_a = \mu_i (1 + K_a) \quad (51)$$

and  $F_{\min}$  for band  $i + 1$  is

$$F_{\min}^{i+1} = \mu_{i+1} - \frac{1}{2}\Delta F_{i+1} = \mu_{i+1} - \mu_{i+1} K_a = \mu_{i+1} (1 - K_a) \quad (52)$$

We want these two values to coincide, therefore

$$\mu_{i+1} = \mu_i \frac{1 + K_a}{1 - K_a} \quad (53)$$

Thus, the peak frequencies follow a geometric series

$$\mu_i = \mu_1 R^{i-1} \quad (54)$$

where

$$R = \frac{1 + K_a}{1 - K_a} \quad (55)$$

## 10.1 Example

If we use the standard values for simple cell median bandwidths from macaque striate cortex:

- $\Delta F = 1.4$  octaves.

- $\Delta\omega = 40$  degrees.

Then,

$$K_a = \frac{2^{\Delta F} - 1}{2^{\Delta F} + 1} = 0.45040 \quad (56)$$

$$K_b = \tan\left(\frac{1}{2}\Delta\omega\right) = 0.36397 \quad (57)$$

$$a = \mu_i \frac{K_a}{C} = 0.9589 \mu_i \quad (58)$$

$$\lambda = \frac{a}{b} = \frac{K_a}{K_b} = 1.23746 \quad (59)$$

$$b = a\lambda = 1.1866 \mu_i \quad (60)$$

$$R = \frac{1 + K_a}{1 - K_a} = 2.6390 \quad (61)$$

Suppose we want three frequency bands and we want the  $F_0$  of the third band to be 0.25. Then,

$$\mu_1 = \frac{0.25}{2.6390^2} = 0.03589 \quad (62)$$

and

$$\frac{1}{2}\Delta F_1 = K_a \mu_1 = 0.01617 \quad (63)$$

Thus, the half magnitude interval<sup>9</sup> is (0.01973, 0.05207)

The second band peaks at

$$\mu_2 = \mu_1 R = 0.09473 \quad (64)$$

and

$$\frac{1}{2}\Delta F_2 = K_a \mu_2 = 0.04267 \quad (65)$$

Thus, the half magnitude interval is (0.05207, 0.1374)

Finally, the third band peaks at

$$\mu_3 = \mu_2 R = 0.2500 \quad (66)$$

and

$$\frac{1}{2}\Delta F_3 = K_a \mu_3 = 0.1126 \quad (67)$$

Thus, the half magnitude interval is (0.1374, 0.3626)

These three Gabors cover the frequency bands of (0.01973, 0.3626)

---

<sup>9</sup>The half magnitude interval here is the frequency coverage of that Gabor in terms of half-magnitude profile:  $\left(\mu_i - \frac{1}{2}\Delta F_i, \mu_i + \frac{1}{2}\Delta F_i\right)$

## 11 Appendix

### 11.1 Fourier transform of the Gabor function

#### 11.1.1 The integral of the Gaussian

Let  $I$  denote the integral

$$I \equiv \int_{-\infty}^{\infty} \exp(-\pi x^2) dx = \int_{-\infty}^{\infty} \exp(-\pi y^2) dy \quad (68)$$

Then,

$$\begin{aligned} I^2 &= \int_{-\infty}^{\infty} \exp(-\pi x^2) dx \int_{-\infty}^{\infty} \exp(-\pi y^2) dy \\ &= \int_{-\infty}^{\infty} \int_{-\infty}^{\infty} \exp(-\pi(x^2 + y^2)) dx dy \end{aligned} \quad (69)$$

Using a polar coordinates  $r$  and  $\varphi$ , this equation can be rewritten as:

$$\begin{aligned} I^2 &= \int_0^{\infty} \int_0^{2\pi} \exp(-\pi r^2) r dr d\varphi \\ &= \int_0^{\infty} 2\pi r \exp(-\pi r^2) dr \\ &= [-\exp(-\pi r^2)]_0^{\infty} \\ &= 1 \end{aligned} \quad (70)$$

Accordingly,

$$I = \int_{-\infty}^{\infty} \exp(-\pi x^2) dx = 1 \quad (71)$$

#### 11.1.2 Fourier transform of the Gaussian

The Fourier transform of the simple 1-D Gaussian is

$$\begin{aligned} &\int_{-\infty}^{\infty} \exp(-\pi x^2) \exp(-2\pi j f x) dx \\ &= \int_{-\infty}^{\infty} \exp(-\pi(x + j f)^2 - \pi f^2) dx \\ &= \exp(-\pi f^2) \int_{-\infty}^{\infty} \exp(-\pi x'^2) dx' \quad (x' \equiv x + j f) \\ &= \exp(-\pi f^2) \end{aligned} \quad (72)$$

In the same way, the Fourier transform of the simple 2-D Gaussian is

$$\begin{aligned} &\int_{-\infty}^{\infty} \int_{-\infty}^{\infty} \exp(-\pi(x^2 + y^2)) \exp(-2\pi j u x) \exp(-2\pi j v y) dx dy \\ &= \int_{-\infty}^{\infty} \exp(-\pi x^2) \exp(-2\pi j u x) dx \int_{-\infty}^{\infty} \exp(-\pi y^2) \exp(-2\pi j v y) dy \\ &= \exp(-\pi u^2) \exp(-\pi v^2) \\ &= \exp(-\pi(u^2 + v^2)) \end{aligned} \quad (73)$$

and so on. More generally,

$$\int_{-\infty}^{\infty} \exp(-\pi x^T x) \exp(-2\pi j u^T x) dx = \exp(-\pi u^T u) \quad (74)$$

That is, the Fourier transform of an N-dimensional Gaussian is also an N-dimensional Gaussian.

### 11.1.3 Several properties of the Fourier transform

Several properties of the Fourier transform will be introduced in this section. Let  $\hat{f}(u)$  denote the Fourier transform of a function  $f(x)$ , i.e.

$$\int_{-\infty}^{\infty} f(x) \exp(-2\pi j u^T x) dx = \hat{f}(u) \quad (75)$$

Then,

$$\begin{aligned} & \int_{-\infty}^{\infty} f(x - x_0) \exp(-2\pi j u^T x) dx \\ &= \exp(-2\pi j u^T x_0) \int_{-\infty}^{\infty} f(x - x_0) \exp(-2\pi j u^T (x - x_0)) dx \\ &= \exp(-2\pi j x_0^T u) \int_{-\infty}^{\infty} f(x') \exp(-2\pi j u^T x') dx' \quad (x' \equiv x - x_0) \end{aligned} \quad (76)$$

$$= \exp(-2\pi j x_0^T u) \hat{f}(u)$$

and also,

$$\begin{aligned} & \int_{-\infty}^{\infty} f(Ax) \exp(-2\pi j u^T x) dx \\ &= \int_{-\infty}^{\infty} f(Ax) \exp(-2\pi j u^T A^{-1} Ax) dx \\ &= \int_{-\infty}^{\infty} f(x') \exp(-2\pi j (A^{-T} u)^T x') \frac{1}{\|A\|} dx' \quad (x' \equiv Ax) \\ &= \frac{1}{\|A\|} \hat{f}(A^{-T} u) \end{aligned} \quad (77)$$

### 11.1.4 Fourier transform of the Gabor function

Here, we have the simple Gaussian envelop and sinusoidal carrier:

$$w(x) = \exp(-\pi x^T x) \quad (78)$$

$$s(x) = \exp(j(2\pi u_0^T x + P))$$

Now we want a Fourier transform of the following Gabor function,

$$\begin{aligned} g(x) &= K w(A(x - x_0)) (s(x) - C) \\ &= K w(A(x - x_0)) (\exp(j(2\pi u_0^T x + P)) - C) \end{aligned} \quad (79)$$



where  $K$  and  $C$  are constants.

Given this function, its Fourier transform will be

$$\begin{aligned}\hat{g}(u) &= \int_{-\infty}^{\infty} g(x) \exp(-2\pi j u^T x) dx \\ &= K \exp(jP) \int_{-\infty}^{\infty} w(A(x - x_0)) \exp(-2\pi j (u - u_0)^T x) dx \\ &\quad - KC \int_{-\infty}^{\infty} w(A(x - x_0)) \exp(-2\pi j u^T x) dx\end{aligned}\quad (80)$$

Using the previously introduced properties, we can see

$$\begin{aligned}\hat{g}(u) &= K \exp(jP) \exp(-2\pi j x_0^T (u - u_0)) \frac{1}{\|A\|} \hat{w}(A^{-T}(u - u_0)) \\ &\quad - KC \exp(-2\pi j x_0^T u) \frac{1}{\|A\|} \hat{w}(A^{-T}u) \\ &= \frac{K}{\|A\|} \exp(-2\pi j x_0^T (u - u_0)) \\ &\quad (\exp(jP) \hat{w}(A^{-T}(u - u_0)) - C \exp(-2\pi j x_0^T u_0) \hat{w}(A^{-T}u))\end{aligned}\quad (81)$$

Remember that  $C$  is a constant that compensates the DC component of the Gabor function, which means  $\hat{g}(0)$  must be equal to 0. Therefore,

$$C = \exp(j(2\pi x_0^T u_0 + P)) \hat{w}(-A^{-T}u_0) \quad (82)$$

then

$$\begin{aligned}g(x) &= K w(A(x - x_0)) \exp(j(2\pi u_0^T x_0 + P)) \\ &\quad (\exp(2\pi j u_0^T (x - x_0)) - \hat{w}(-A^{-T}u_0))\end{aligned}\quad (83)$$

and

$$\begin{aligned}\hat{g}(u) &= \frac{K}{\|A\|} \exp(j(-2\pi x_0^T (u - u_0) + P)) \\ &\quad (\hat{w}(A^{-T}(u - u_0)) - \hat{w}(-A^{-T}u_0) \hat{w}(A^{-T}u))\end{aligned}\quad (84)$$

Using the following definitions:

$$\begin{aligned}w(x) &= \exp(-\pi x^T x) \\ \hat{w}(u) &= \exp(-\pi u^T u)\end{aligned}\quad (85)$$

we can get

$$\begin{aligned}g(x) &= K \exp(-\pi (x - x_0)^T A^T A (x - x_0)) \exp(j(2\pi u_0^T x_0 + P)) \\ &\quad (\exp(2\pi j u_0^T (x - x_0)) - \exp(-\pi u_0^T A^{-1} A^{-T} u_0))\end{aligned}\quad (86)$$

and

$$\begin{aligned}\hat{g}(u) &= \frac{K}{\|A\|} \exp(j(-2\pi x_0^T (u - u_0) + P)) \\ &\quad (\exp(-\pi (u - u_0)^T A^{-1} A^{-T} (u - u_0)) \\ &\quad - \exp(-\pi u_0^T A^{-1} A^{-T} u_0) \exp(-\pi u^T A^{-1} A^{-T} u))\end{aligned}\quad (87)$$

In order to have the generalized 2-D Gabor function, consider  $A \equiv DV$ , where  $D$  is a diagonal matrix and  $V$  is a rotation matrix such that

$$D = \begin{pmatrix} a & 0 \\ 0 & b \end{pmatrix}, \quad V = \begin{pmatrix} \cos \theta & \sin \theta \\ -\sin \theta & \cos \theta \end{pmatrix} \quad (88)$$

Then, admissible 2-D Gabor function is introduced:

$$\begin{aligned} g(x, y) = & K \exp \left( -\pi \left( a^2 (x - x_0)_r^2 + b^2 (y - y_0)_r^2 \right) \right) \exp \left( j \left( 2\pi (u_0 x_0 + v_0 y_0) + P \right) \right) \\ & \left( \exp \left( 2\pi j (u_0 (x - x_0) + v_0 (y - y_0)) \right) - \exp \left( -\pi \left( \frac{u_{0r}^2}{a^2} + \frac{v_{0r}^2}{b^2} \right) \right) \right) \end{aligned} \quad (89)$$

And its Fourier transform is:

$$\begin{aligned} \hat{g}(u, v) = & \frac{K}{ab} \exp \left( j \left( -2\pi (x_0 (u - u_0) + y_0 (v - v_0)) + P \right) \right) \\ & \left( \exp \left( -\pi \left( \frac{(u - u_0)_r^2}{a^2} + \frac{(v - v_0)_r^2}{b^2} \right) \right) \right. \\ & \left. - \exp \left( -\pi \left( \frac{u_{0r}^2}{a^2} + \frac{v_{0r}^2}{b^2} \right) \right) \exp \left( -\pi \left( \frac{u_r^2}{a^2} + \frac{v_r^2}{b^2} \right) \right) \right) \end{aligned} \quad (90)$$

## 11.2 Another formula of the Gabor function

In other papers, you may see another formula representation of the Gabor function. For example, in most papers,  $x_0 = y_0 = 0, P = 0$ . Then,

$$\begin{aligned} g(x, y) = & K \exp \left( -\pi \left( a^2 x_r^2 + b^2 y_r^2 \right) \right) \\ & \left( \exp \left( 2\pi j (u_0 x + v_0 y) \right) - \exp \left( -\pi \left( \frac{u_{0r}^2}{a^2} + \frac{v_{0r}^2}{b^2} \right) \right) \right) \end{aligned} \quad (91)$$

$$\begin{aligned} \hat{g}(u, v) = & \frac{K}{ab} \left( \exp \left( -\pi \left( \frac{(u - u_0)_r^2}{a^2} + \frac{(v - v_0)_r^2}{b^2} \right) \right) \right. \\ & \left. - \exp \left( -\pi \left( \frac{u_{0r}^2}{a^2} + \frac{v_{0r}^2}{b^2} \right) \right) \exp \left( -\pi \left( \frac{u_r^2}{a^2} + \frac{v_r^2}{b^2} \right) \right) \right) \end{aligned} \quad (92)$$

Moreover,  $a = b \equiv \sigma$  in some paper. The rotation angle has no effect ( $\theta = 0$ ) in this case.

$$\begin{aligned} g(x, y) = & K \exp \left( -\pi \sigma^2 (x^2 + y^2) \right) \\ & \left( \exp \left( 2\pi j (u_0 x + v_0 y) \right) - \exp \left( -\frac{\pi}{\sigma^2} (u_0^2 + v_0^2) \right) \right) \end{aligned} \quad (93)$$

$$\begin{aligned} \hat{g}(u, v) = & \frac{K}{\sigma^2} \left( \exp \left( -\frac{\pi}{\sigma^2} ((u - u_0)^2 + (v - v_0)^2) \right) \right. \\ & \left. - \exp \left( -\frac{\pi}{\sigma^2} (u_0^2 + v_0^2) \right) \exp \left( -\frac{\pi}{\sigma^2} (u^2 + v^2) \right) \right) \end{aligned} \quad (94)$$

Then if you restrict the magnitude of spatial frequency of the sinusoidal carrier  $F_0$  to satisfy this equation:

$$F_0 = \sqrt{u_0^2 + v_0^2} = \frac{\sigma^2}{\sqrt{2\pi}} \quad (95)$$

the Gabor function will be

$$g(x, y) = K \exp(-\pi\sigma^2(x^2 + y^2)) \left( \exp\left(j\sqrt{2\pi}\sigma^2(x \cos \omega_0 + y \sin \omega_0)\right) - \exp\left(-\frac{\sigma^2}{2}\right) \right) \quad (96)$$

$$\hat{g}(u, v) = \frac{K}{\sigma^2} \left( \exp\left(-\frac{\pi}{\sigma^2}((u - u_0)^2 + (v - v_0)^2)\right) - \exp\left(-\frac{\sigma^2}{2}\right) \exp\left(-\frac{\pi}{\sigma^2}(u^2 + v^2)\right) \right) \quad (97)$$

Finally if you use  $K = 2\pi\sigma^2$ ,

$$g(x, y) = 2\pi\sigma^2 \exp(-\pi\sigma^2(x^2 + y^2)) \left( \exp\left(j\sqrt{2\pi}\sigma^2(x \cos \omega_0 + y \sin \omega_0)\right) - \exp\left(-\frac{\sigma^2}{2}\right) \right) \quad (98)$$

$$\hat{g}(u, v) = 2\pi \left( \exp\left(-\frac{\pi}{\sigma^2}((u - u_0)^2 + (v - v_0)^2)\right) - \exp\left(-\frac{\sigma^2}{2}\right) \exp\left(-\frac{\pi}{\sigma^2}(u^2 + v^2)\right) \right) \quad (99)$$

Additionally, you can use angular frequency  $(\nu, \xi)$  instead of  $(u, v)$ . Then,

$$g(x, y) = 2\pi\sigma^2 \exp\left(-\pi\sigma^2(x^2 + y^2)\right) \left( \exp(j(\nu_0 x + \xi_0 y)) - \exp\left(-\frac{\sigma^2}{2}\right) \right) \quad (100)$$

$$\hat{g}(u, v) = 2\pi \left( \exp\left(-\frac{1}{4\pi\sigma^2}((\nu - \nu_0)^2 + (\xi - \xi_0)^2)\right) - \exp\left(-\frac{\sigma^2}{2}\right) \exp\left(-\frac{1}{4\pi\sigma^2}(\nu^2 + \xi^2)\right) \right) \quad (101)$$

In fact, angular frequency representation can be seen in many papers. So it may be useful to have the quite general Gabor function<sup>10</sup> in that format:

$$g(x, y) = K \exp\left(-\pi(a^2 x_r^2 + b^2 y_r^2)\right) \left( \exp(j(\nu_0 x + \xi_0 y)) - \exp\left(-\frac{1}{4\pi} \left( \frac{\nu_{0r}^2}{a^2} + \frac{\xi_{0r}^2}{b^2} \right) \right) \right) \quad (102)$$

$$\hat{g}(u, v) = \frac{K}{ab} \left( \exp\left(-\frac{1}{4\pi} \left( \frac{(\nu - \nu_0)_r^2}{a^2} + \frac{(\xi - \xi_0)_r^2}{b^2} \right) \right) - \exp\left(-\frac{1}{4\pi} \left( \frac{\nu_{0r}^2}{a^2} + \frac{\xi_{0r}^2}{b^2} \right) \right) \exp\left(-\frac{1}{4\pi} \left( \frac{\nu_r^2}{a^2} + \frac{\xi_r^2}{b^2} \right) \right) \right) \quad (103)$$

---

<sup>10</sup>Only  $x_0 = y_0 = 0, P = 0$  are assumed.

## 12 History

- The first version of this document, which was 14 page long, was written by Javier R. Movellan in 1996.
- The document was made open source under the GNU Free Documentation License 1.1 on August 6 2002, as part of the Kolmogorov Project.
- On September 3 2002 we added the changes made by Kenta Kawamoto. These included a 7 page Appendix with sections on the Fourier transform of the Gabor function, and an alternative formula for the Gabor function.
- October 9, 2003. Javier R. Movellan changed the license to GFDL 1.2 and included an endorsement section.

## References

- Adelson, E. H. and Bergen, J. R. (1985). Spatiotemporal energy models for the perception of motion. *Journal of the optical society of america A*, 2:284–299.
- De Valois, R. L., Albrecht, D. G., and Thorell, L. G. (1982a). Spatial frequency selectivity of cells in macaque visual cortex. *Vision Research*, 22:545–559.
- De Valois, R. L., Yund, W., and Hepler, N. (1982b). The orientation and direction selectivity of cells in macaque visual cortex. *Vision Research*, 22:531–544.
- Emerson, R. C., Bergen, J. R., and Adelson, E. H. (1992). Directionally selective complex cells and the computation of motion energy in cat visual cortex. *Vision Research*, 32(2):203–218.
- Heeger, D. (1991). Nonlinear model of neural responses in cat visual cortex. In Landy, M. and Movshon, J., editors, *Computational Models of Visual Processing*, pages 119–133. MIT Press, Cambridge, MA.
- Jones, J. P. and Palmer, L. (1987). An evaluation of the two-dimensional gabor filter model of simple receptive fields in cat striate cortex. *Journal of Neurophysiology*, 58:1233–1258.
- Morrone, M. C., Burr, D. C., and Maffei, L. (1982). Functional significance of cross-orientation inhibition, part I. *Neurophysiology. Proc. R. Soc. Lond. B*, 216:335–354.
- Movshon, J. A., Thompson, I. D., and Tolhurst, D. J. (1987). Receptive field organization of complex cells in the cat’s striate cortex. *Journal of Physiology (London)*, 283:53–77.
- Pollen, D. A. and Ronner, S. F. (1981). Phase relationships between adjacent simple cells in the visual cortex. *Science*, 212:1409–1411.